

Robust digital optimal control on IBM’s quantum computers

Meri Harutyunyan,¹ Frédéric Holweck,^{1,2} Dominique Sugny,¹ and Stéphane Guérin^{1,*}

¹Laboratoire Interdisciplinaire Carnot de Bourgogne, UMR CNRS 6303,

Université de Bourgogne Franche-Comté, BP 47870, F-21078 Dijon, France

²Department of Mathematics and Statistics, Auburn University, Auburn, AL, USA

(Dated: October 18, 2022)

The ability of pulse-shaping devices to generate accurately quantum optimal control is a strong limitation to the development of quantum technologies. We propose and demonstrate a systematic procedure to design robust digital control processes adapted to such experimental constraints. We show to what extent this digital pulse can be obtained from its continuous-time counterpart. A remarkable efficiency can be achieved even for a limited number of pulse parameters. We experimentally implement the protocols on IBM’s quantum computers for a single qubit, obtaining an optimal robust transfer in a time $T = 382$ ns.

Introduction. Operating quantum technologies requires fast and accurate control of quantum systems [1, 2]. Optimal control allows one to drive in principle the dynamics at the quantum speed limit [3]. In a two-level system, one can show that it coincides with a resonant square π -pulse [4]. However, the final result depends on the quality of the pulse: deviations of the amplitude (or of the time of interaction), referred to as pulse inhomogeneities, of order ε leads to an error of the same order for quantum gate and of order ε^2 for population transfer. Improving robustness is thus vital to provide ultrahigh-fidelity quantum information processing.

Adiabatic passage technique allows such robustness but at the cost of slow and inexact dynamics [5–7]. Composite pulses, made of a π -pulse sequence with well-defined phases, are a powerful and simple tool for robust control [8–13] even if they are not optimal in terms of control time or energy used. Composite pulses have been recently implemented on IBM’s computers [14]. Robust optimal control protocols have been derived using gradient-based algorithms (such as GRAPE [15, 16]) or directly from the Pontryagin’s Maximum Principle [17, 18]. Alternative methods based on inverse engineering geometric control have been also recently proposed [19, 20], where the controls are determined from a shaped trajectory in the dynamical parameter space, for instance on the Bloch sphere. The latter, referred to as robust inverse optimization (RIO) [20, 21], is derived from shortcut to adiabaticity techniques [22–24]. It combines the robustness of composite pulses, formulated as constraint integrals for a given order, with time-optimality. In the case of pulse inhomogeneities, the control has constant amplitude but features a time-continuous phase modulation.

Robustness to variations in system parameters is not the only key limitation to the experimental implementation of control protocols. Another hurdle relates to the ability of pulse-shaping devices to generate the theoretically designed driving process. With the notable exception of composite pulses, the majority of studies has assumed that the amplitude or phase (or both) of the

control can vary continuously over time. While this assumption is natural in experiments where arbitrary waveform generators are available, this procedure is problematic when the hardware is limited, for example, to specific pulse shapes and thus to a finite number of control parameters. At this stage, a numerical solution can be found by starting from the most general pulse shape and optimizing the corresponding free parameters [25]. However, this approach is not ideal because it generally prevents any analytical or geometric study and it makes numerical optimization more difficult by increasing the number of traps in the control landscape [26].

We propose in this Letter a general procedure to overcome these two limitations, demonstrated in the case of a one-qubit robust control. In view of an experimental proof of principle, we consider below specifically the case of the RIO technique on IBM’s quantum computers [28], based on superconducting transmon qubits. We stress that the same approach could be used with other optimized control and to more complex systems, but this example has the advantage of highlighting that geometric properties can still be used in this constrained control problem. Instead of producing continuous time-dependent phase, which is a relatively difficult practical task in such systems [29], we develop a simpler and efficient digital version (referred to as DRIO). Digital control has been originally proposed and explored in the context of adiabatic passage with a series of femtosecond pulses [30] and in the context of stimulated Raman passage, adiabatic [31] or not [32], with application in spatial adiabatic passage [33]. In DRIO, the control phase is varied digitally (or in a piecewise way), produced with a short pulse series, where each pulse constituent features a constant phase. This shares similarity with composite pulses but with the important difference that one uses subpulses of small area (much smaller than π): The total pulse area is optimal (i.e. time-optimal for a given peak amplitude), and thus always smaller by construction than its composite counterpart for the same robustness order.

Theory of digital control. We consider a two-state system driven by a train of resonant pulses of delay τ , where each individual pulse n features the same shape $0 \leq \Lambda(t) \leq 1$, of characteristic duration σ , but has arbitrary phase φ_n and peak amplitude Ω_n . The two-state

*Electronic address: sguerin@u-bourgogne.fr

Hamiltonian reads in the rotating wave approximation (RWA) and in the basis of bare states (in units such that $\hbar = 1$)

$$\hat{H}(t) = \frac{1}{2} \sum_n \Omega_n \mathbf{1}_n(t) \Lambda\left(\frac{t-t_n}{\sigma}\right) \begin{bmatrix} 0 & e^{-i\varphi_n} \\ e^{i\varphi_n} & 0 \end{bmatrix} \quad (1)$$

with pulses centered in $t_n = n\tau$. We denote the indicator function on the interval I_n : $\mathbf{1}_n(t) = 1$ if $t \in I_n \equiv [t_{n-\frac{1}{2}}, t_{n+\frac{1}{2}}]$; 0 otherwise.

We consider smooth pulses, such as for instance Gaussian of the form $\Lambda(t) = e^{-t^2}$, that do not overlap, $\sigma \ll \tau$. Typically, one can take $\tau = 6\sigma$ for the Gaussian pulses. In that situation, one can safely omit the indicator function from Hamiltonian (1) to which we associate the propagator $\hat{U}(t, t_i)$ (with t_i the initial time).

The integer n labeling the pulses in the train runs in principle from $-\infty$ to $+\infty$, i.e. $n = 0$ corresponds to the central pulse, and the peak Rabi frequency of the pulse n is constructed from a continuous shape $0 \leq \Pi(t) \leq 1$ that is sampled as

$$\Omega_n = \Omega_0 \Pi(t_n/T), \quad (2)$$

where T denotes its characteristic duration. One can choose for instance a smooth Gaussian shape $\Pi(t) = e^{-t^2}$ for implementing digital adiabatic passage, or a constant (square) pulse $\Pi(t) = 1$ as it will be the case for DRIO. The phases φ_n form a piecewise constant function whose value varies from pulse to pulse with the same timescale as the peak Rabi frequency

$$\varphi_n = \varphi(t_n) \equiv \tilde{\varphi}(t_n/T). \quad (3)$$

We show below that this digital model (1) can be made approximately equivalent to an effective continuous Hamiltonian, see (16). The general strategy is thus to derive the peak Rabi frequencies Ω_n and the phases φ_n from the analysis of the continuous model.

Since the phase is constant for each pulse, one can alternatively consider the Hamiltonian

$$\hat{H}_\delta(t) = \frac{1}{2} \sum_n A_n \delta(t-t_n) \begin{bmatrix} 0 & e^{-i\varphi_n} \\ e^{i\varphi_n} & 0 \end{bmatrix}, \quad (4)$$

associated to the propagator $\hat{U}_\delta(t, t_i)$, where the Gaussian pulse area $A_n = \Omega_n \int_{t_{n-\frac{1}{2}}}^{t_{n+\frac{1}{2}}} dt \Lambda\left(\frac{t-t_n}{\sigma}\right) = \sqrt{\pi}\sigma\Omega_n$ between $t_{n\pm\frac{1}{2}} = (n \pm \frac{1}{2})\tau$ is concentrated into a Dirac δ pulse. One can indeed connect the propagators

$$\hat{U}(t_{n+\frac{1}{2}}, t_{n-\frac{1}{2}}) = \hat{U}_\delta(t_{n+\frac{1}{2}}, t_{n-\frac{1}{2}}) = \hat{U}_\delta(t_n^+, t_n^-) \quad (5a)$$

$$= \begin{bmatrix} \cos(A_n/2) & -ie^{-i\varphi_n} \sin(A_n/2) \\ -ie^{i\varphi_n} \sin(A_n/2) & \cos(A_n/2) \end{bmatrix} \quad (5b)$$

with t_n^\pm denoting times immediately before and after $t_n = n\tau$, respectively. We highlight the fact that there is no additional phase coming from the timeshifts $t_{n+\frac{1}{2}} \rightarrow t_n^+$ and $t_{n-\frac{1}{2}} \rightarrow t_n^-$ since the diagonal elements of the Hamiltonian are zero.

In the next step, we incorporate the phases in the wavefunction applying the piecewise constant transformation

$$T(t) = \begin{bmatrix} e^{-i\sum_n \mathbf{1}_n(t)\varphi_n/2} & 0 \\ 0 & e^{i\sum_n \mathbf{1}_n(t)\varphi_n/2} \end{bmatrix}, \quad (6)$$

which leaves unchanged the population of the states. We obtain

$$\begin{aligned} H_\delta &\equiv T^\dagger \hat{H}_\delta T - iT^\dagger \frac{dT}{dt} = \\ &= \frac{1}{2} \sum_n \begin{bmatrix} -\delta(t-t_{n-\frac{1}{2}}) \Delta\varphi_n & \delta(t-t_n) A_n \\ \delta(t-t_n) A_n & \delta(t-t_{n-\frac{1}{2}}) \Delta\varphi_n \end{bmatrix} \end{aligned} \quad (7)$$

with

$$\Delta\varphi_n = \varphi_n - \varphi_{n-1} \quad (8)$$

and the corresponding solution $\phi(t) = T^\dagger(t)\Phi(t)$ with $\Phi(t)$ the state solution of the original problem (but with the Dirac δ pulses): $\Phi(t_n^+) = \hat{U}_\delta(t_n^+, t_n^-)\Phi(t_n^-)$, i.e.

$$\Phi(t) = \hat{U}_\delta(t, t_i)\Phi(t_i) = T(t)U_\delta(t, t_i)T^\dagger(t_i)\Phi(t_i). \quad (9)$$

The Hamiltonian (7) is characterized by the superposition of two time-shifted trains of coupling and detuning terms.

When $\Omega_n \equiv \Omega_0$ and $\varphi_n \equiv \varphi_0$ are constant for any n , i.e. $\Delta\varphi_n = 0$, the interaction is strictly periodic if one considers an infinite number of pulses and the Hamiltonian reads

$$H_\delta = \frac{A_0}{2\tau} \begin{bmatrix} 0 & 1 \\ 1 & 0 \end{bmatrix} \sum_k e^{ik\gamma t} \quad (10)$$

with the frequency of the pulse repetition $\gamma = 2\pi/\tau$. We have here used the Poisson formula for the Dirac distribution leading to the spectral representation of the Dirac comb, $\sum_n \delta(t-n\tau) = \frac{1}{\tau} \sum_k e^{ik\gamma t}$. When Ω_n and φ_n vary as functions of n , one can use the sampling property, $\sum_n f(n\tau)\delta(t-n\tau) = f(t) \sum_n \delta(t-n\tau)$, for a function $f(t)$, which leads to the Hamiltonian

$$H_\delta = \frac{1}{2\tau} \sum_k \begin{bmatrix} -e^{i\pi k} \Delta\varphi(t) & A(t) \\ A(t) & e^{i\pi k} \Delta\varphi(t) \end{bmatrix} e^{ik\gamma t} \quad (11)$$

such that $\Delta\varphi(t_{n-\frac{1}{2}}) = \Delta\varphi_n$, $A(t_n) = A_n$. If one considers piecewise constant peak Rabi frequencies of the form (2), it is natural to take for Gaussian subpulses

$$A(t) = \sqrt{\pi}\sigma\Omega_0\Pi(t/T). \quad (12)$$

For the detuning, one can determine a function from backward and forward Taylor expansions of the phase (3) at time $t_{n-\frac{1}{2}}$

$$\begin{aligned} \varphi_n &= \varphi(t_n) = \varphi(t_{n-\frac{1}{2}}) + \frac{\tau}{2}\varphi'(t_{n-\frac{1}{2}}) + \dots \\ \varphi_{n-1} &= \varphi(t_{n-1}) = \varphi(t_{n-\frac{1}{2}}) - \frac{\tau}{2}\varphi'(t_{n-\frac{1}{2}}) + \dots \end{aligned}$$

i.e.

$$\begin{aligned} \Delta\varphi(t_{n-\frac{1}{2}}) &= \tau\varphi'(t_{n-\frac{1}{2}}) + \frac{1}{3}\left(\frac{\tau}{2}\right)^3\varphi'''(t_{n-\frac{1}{2}}) + \dots \\ &+ \frac{2}{(2p+1)!}\left(\frac{\tau}{2}\right)^{2p+1}\varphi^{(2p+1)}(t_{n-\frac{1}{2}}) + \dots \end{aligned} \quad (13)$$

where $p \geq 0$ is an integer. At this stage, no approximation has been made in Hamiltonian (11), whatever the variations of $\Delta\varphi(t)$ and $A(t)$ are, when one considers an infinite number of pulses, i.e. $T \gg \tau$. The timescales of the digital control need thus to satisfy

$$\sigma \ll \tau \ll T. \quad (14)$$

The Hamiltonian (11) is not piecewise anymore, but it contains an infinite number of modes with the same amplitude $A(t)/2\tau$. The mode $k = 0$ is near resonant while the other ones can be considered as perturbation in the weak-field limit. At the lowest approximation, one only takes into account the resonant term $k = 0$, that we refer to as the second RWA. It can be applied when

$$A(t) \ll \sqrt{4\pi^2 - \Delta\varphi(t)^2}. \quad (15)$$

This leads to the resonant effective Hamiltonian, derived from (11) for $k = 0$

$$H_{\delta,0} = \frac{1}{2\tau} \begin{bmatrix} -\Delta\varphi(t) & A(t) \\ A(t) & \Delta\varphi(t) \end{bmatrix} \equiv \frac{1}{2} \begin{bmatrix} -\Delta & \Omega \\ \Omega & \Delta \end{bmatrix}. \quad (16)$$

This effective Hamiltonian includes an effective detuning $\Delta \equiv \Delta\varphi(t)/\tau$ and an effective Rabi frequency corresponding to the original piecewise Rabi frequency area divided by τ , $\Omega \equiv A(t)/\tau$. This effective Hamiltonian (16) can be analysed from standard techniques. For instance, if one considers adiabatic passage, it is more efficient when $\int A(t)dt \equiv \sqrt{\pi}\sigma\Omega_0T \int \Lambda(s)ds \gg \tau$, and for a sufficiently slow evolution of the detuning.

Digital robust inverse optimization. We consider robust inverse optimization (RIO), where robustness is imposed with respect to pulse inhomogeneities (i.e. amplitude and/or width) and optimization with respect to pulse duration, i.e in minimum time (for a given pulse peak). At third order, the solution is a constant pulse of amplitude Ω and duration $T = 1.86\pi/\Omega$ and a detuning of Jacobi elliptic cosine form

$$\Delta = \Delta_0 \operatorname{cn}(\omega(t - t_i) + K(m), m), \quad t \in [0, T] \quad (17)$$

with, the initial time t_i , and, for the problem of complete population transfer, $m = 0.235$, $\omega = 1.149\Omega$, and $\Delta_0 = 1.114\Omega$.

The peak amplitudes of the pulses are constant $\Omega_n = \Omega_0$, since given by (2) where $\Pi(t) = 1$, with the Rabi coupling Ω_0 given by (12), $\Omega_0 = \tau\Omega/\sqrt{\pi}\sigma$. We consider a large number N of pulses, typically $N = 15$, giving the full duration $T = N\tau$, i.e. $\Omega_0 = T\Omega/\sqrt{\pi}N\sigma$. We use for the delay $\tau = 6\sigma$, i.e. $\Omega_0 = 6T\Omega/\sqrt{\pi}N\tau$. The phase $\varphi(t)$ is solution of (13), extended at all times:

$$\Delta = \varphi' + \frac{\tau^2}{24}\varphi''' + \dots = \varphi'[1 + O((\tau/T)^2)] \approx \varphi'. \quad (18)$$

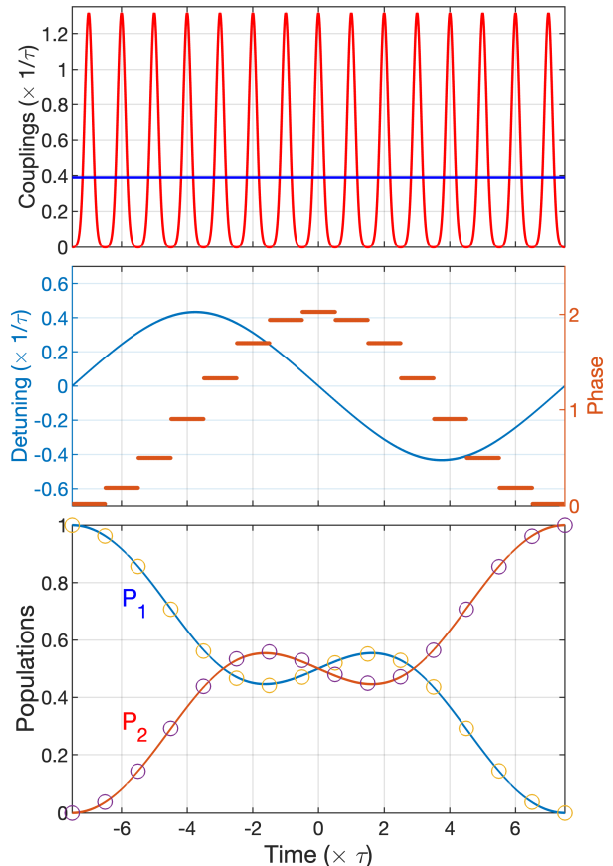


FIG. 1: (Color online) Digital and continuous third-order RIO with $N = 15$. τ is the delay between the pulses and the full duration is $T = N\tau$. Upper frame: the Rabi frequency pulse series of peak amplitude Ω_0 and the corresponding continuous constant Rabi frequency Ω . Middle frame: the digital (piecewise) phases and the corresponding detuning. Lower frame: Population dynamics from the effective continuous model (16) (full line) and at the beginning and the end of each constituent pulse of the digital model (1) (circles), showing complete population transfers (exactly for continuous RIO, and with an error of less than 10^{-4} for DRIO). The total pulse area is 1.86π for both models.

It is next digitalized at times t_n when the pulses reach their peak value.

Figure 1 shows the dynamics of the continuous and digital RIO for $N = 15$. DRIO achieves a very good accuracy with an error in population transfer less than 10^{-4} . A time-optimal protocol of fifth-order robustness with respect to pulse inhomogeneities can be derived by following the techniques described in Ref. [20]. It gives a constant pulse of amplitude Ω and duration $T = 2.71\pi/\Omega$. The dynamics are shown in Fig. 2.

Experimental results. We performed the experiments of the robustness profiles using IBM Quantum Experience [28]. It is built with superconducting transmon qubits, which can be controlled by microwave pulses. We

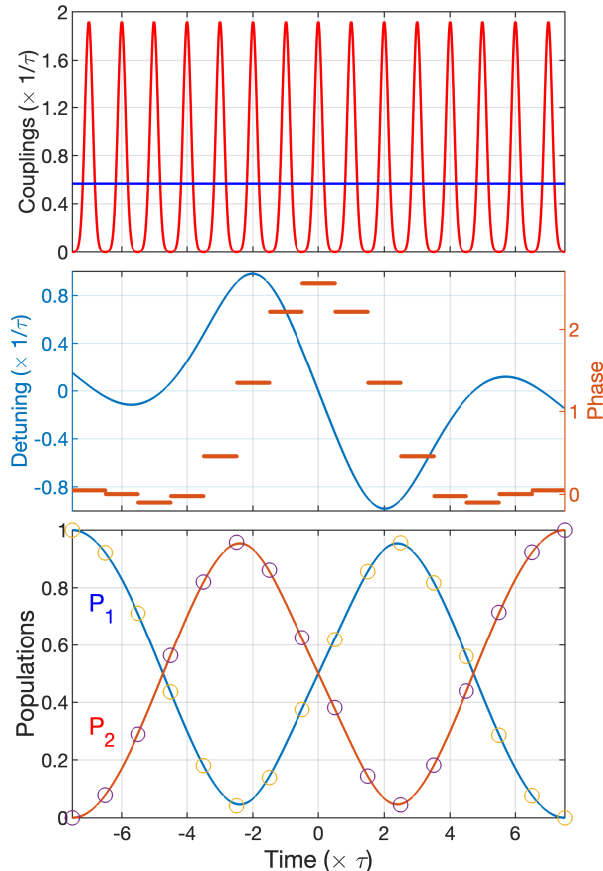


FIG. 2: (Color online) Same as Fig. 1, but for the fifth-order RIO and DRIO, of total pulse area 2.71π .

used the low-level quantum computing Qiskit Pulse [34], as a module of the open-source framework Qiskit [35]. The processor used is *ibmq_manila*, which is one of the IBM five-qubit Falcon Processors (Falcon r5.11L). Note that one obtained the same final result for the other five-qubit systems of the IBM Quantum Experience.

The parameters of the qubit, calibrated at the time of the experiment, are the following: qubit transition frequency of 4.971 GHz, anharmonicity of -0.34378 GHz, T_1 and T_2 coherence times of $153.89 \mu\text{s}$ and $46.19 \mu\text{s}$, respectively, and readout error of 3% (all are averaged values). We performed each experiment applying a sequence of Gaussian pulses with the appropriate phase shifts, according to Fig. 1 and 2, respectively, where each single pulse has a duration of $\sigma = 3 \times \sqrt{2}$ ns. The total duration of the full process is $T = 382$ ns. In our figures we have plotted the transition probability as a function of the deviation $-1 \leq \alpha \leq 1$ from the theoretical optimal value, $\Omega \rightarrow \Omega(1 + \alpha)$, with $\Omega = 1.86\pi/T$ (i.e. 15.3 MHz) and $\Omega = 2.71\pi/T$ (i.e. 22.3 MHz) for the third-order and fifth-order robustness, respectively. Each point corresponds to an experiment repeated 1024 times. We have checked that the experimental result

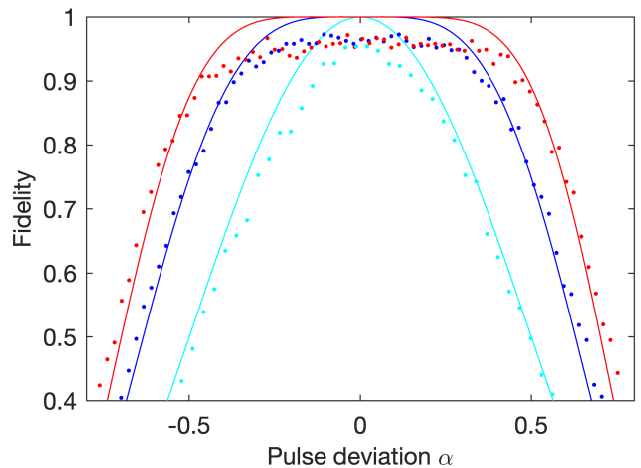


FIG. 3: (Color online) Experimental (dotted lines) digital π -pulse (light blue), third- (dark blue) and fifth-order (red) DRIO robustness profile as a function of the relative pulse amplitude deviation α , compared to their theoretical predictions (full lines).

does not depend on the ratio σ/τ and slightly on the repetition number that can vary from 1024 to 8096 times.

The experimental profiles of the single (square) Rabi pulse, the third- and fifth-order DRIO are shown in Fig. 3. A reasonable match between theory and experiment is achieved. The small discrepancy amounts to approximately 3%, which corresponds to the measurement error, as published by IBM at the time of the experiment. Apart this error, the excitation profile fits remarkably well the theoretical prediction; the efficiency and robustness of DRIO are clearly demonstrated.

Conclusions. We focus in this study on the experimental implementation of a simple digital optimization control procedure for realizing a robust one-qubit state-to-state transfer based on its time-continuous derivation. This approach has the decisive advantage of being able to account for the limitations of pulse-shaping devices, while using to some extent geometric and numerical properties of time-continuous optimal robust control protocols. We have shown the remarkable accuracy of the digital control, compatible with quantum information ultrahigh fidelity, with a digitalization featuring a number of sub-pulses as low as 15. The next step of this study could be the implementation of one-qubit quantum gates [36] and the control of coupled qubits [37]. In particular, the use of a non-constant pulse amplitude can be similarly implemented by modulating the peaks of the subpulses according to the continuous control. This digital control protocol opens the experimental implementation of optimal driving strategies in complex systems.

Acknowledgments

We acknowledge support from the EUR-EIPHI Graduate School (17-EURE-0002) and from the European Union's Horizon 2020 research and innovation program

under the Marie Skłodowska-Curie Grant No. 765075 (LIMQUET). We acknowledge the use of IBM Quantum services for this work; the views expressed are those of the authors, and do not reflect the official policy or position of IBM.

-
- [1] M.A. Nielsen and I.L. Chuang, Quantum Computation and Quantum Information (Cambridge University Press, Cambridge, U.K., 2000).
- [2] C.P. Koch, U. Boscain, T. Calarco, G. Dirr, S. Filipp, S.J. Glaser, R. Kosloff, S. Montangero, T. Schulte-Herbrüggen, D. Sugny, F.K. Wilhelm, Quantum optimal control in quantum technologies. Strategic report on current status, visions and goals for research in Europe, EPJ Quantum Technol. **9**, 19 (2022).
- [3] T. Caneva, M. Murphy, T. Calarco, R. Fazio, S. Montangero, V. Giovannetti, and G. E. Santoro, Optimal Control at the Quantum Speed Limit, Phys. Rev. Lett. **103**, 240501 (2009).
- [4] U. Boscain, G. Charlot, J.-P. Gauthier, S. Guérin, and H. R. Jauslin, Optimal control in laser-induced population transfer for two- and three-level quantum systems, J. Math. Phys. **43**, 2107 (2002).
- [5] M.M.T. Loy, Observation of Population Inversion by Optical Adiabatic Rapid Passage, Phys. Rev. Lett. **32**, 814 (1974).
- [6] L.P. Yatsenko, S. Guérin, and H.R. Jauslin, Topology of adiabatic passage, Phys. Rev. A **65**, 043407 (2002).
- [7] N.V. Vitanov, A.A. Rangelov, B.W. Shore, and K. Bergmann, Stimulated Raman adiabatic passage in physics, chemistry, and beyond, Rev. Mod. Phys. **89**, 015006 (2017).
- [8] S. Wimperis, Broadband, Narrowband, and Passband Composite Pulses for Use in Advanced NMR Experiments, J. Magn. Reson. **109**, 221 (1994).
- [9] H.K. Cummins, G. Llewellyn, and J.A. Jones, Tackling Systematic Errors in Quantum Logic Gates with Composite Rotations, Phys. Rev. A **67**, 042308 (2003).
- [10] B.T. Torosov, S. Guérin, and N.V. Vitanov, High-Fidelity Adiabatic Passage by Composite Sequences of Chirped Pulses, Phys. Rev. Lett. **106**, 233001 (2011).
- [11] J.A. Jones, Designing short robust NOT gates for quantum computation, Phys. Rev. A **87**, 052317 (2013).
- [12] B.T. Torosov and N.V. Vitanov, Arbitrarily accurate variable rotations on the Bloch sphere by composite pulse sequences, Phys. Rev. A **99**, 013402 (2019).
- [13] H.L. Gevorgyan and N.V. Vitanov, Ultrahigh-fidelity composite rotational quantum gates, Phys. Rev. A **104**, 012609 (2021).
- [14] B.T. Torosov and N.V. Vitanov, Experimental Demonstration of Composite Pulses on IBM's Quantum Computer, Phys. Rev. Appl. **18**, 034062 (2022).
- [15] N. Khaneja, T. Reiss, C. Kehlet, T. Schulte-Herbrüggen, and S.J. Glaser, Design of NMR pulse sequences by gradient ascent algorithms, J. Magn. Reson. **172**, 296 (2005).
- [16] K. Kozbar, S. Ehni, T. E. Skinner, S. J. Glaser, and B. Luy, Exploring the limits of broadband 90° and 180° universal rotation pulses, J. Magn. Reson. **225**, 142 (2012).
- [17] L. Van Damme, Q. Ansel, S.J. Glaser, and D. Sugny, Robust optimal control of two-level quantum systems, Phys. Rev. A **95**, 063403 (2017).
- [18] U. Boscain, M. Sigalotti and D. Sugny, Introduction to the Pontryagin Maximum Principle for quantum optimal control, PRX Quantum **2**, 030203 (2021).
- [19] J. Zeng, C.H. Yang, A. S. Dzurak, and E. Barnes, Geometric formalism for constructing arbitrary single-qubit dynamically corrected gates, Phys. Rev. A **99**, 052321 (2019).
- [20] G. Dridi, K. Liu, S. Guérin, Optimal robust quantum control by inverse geometric optimization, Phys. Rev. Lett. **125**, 250403 (2020).
- [21] X. Laforgue, G. Dridi and S. Guérin, Optimal robust stimulated Raman exact passage by inverse optimization, Phys. Rev. A **105**, 032807 (2022).
- [22] A. Ruschhaupt, X. Chen, D. Alonso and J. G. Muga, N. J. Phys. **14**, 093040 (2012).
- [23] D. Daems, A. Ruschhaupt, D. Sugny, and S. Guérin, Robust Quantum Control by a Single-Shot Shaped Pulse, Phys. Rev. Lett. **111**, 050404 (2013).
- [24] D. Guéry-Odelin, A. Ruschhaupt, A. Kiely, E. Torrontegui, S. Martínez-Garaot, and J.G. Muga, Shortcuts to adiabaticity: Concepts, methods, and applications, Rev. Mod. Phys. **91**, 045001 (2019).
- [25] T.E. Skinner and N.I. Gershenzon, Optimal control design of pulse shapes as analytic functions, J. Magn. Reson. **204**, 248 (2010).
- [26] K.W. Moore and H. Rabitz, Exploring constrained quantum control landscapes, J. Chem. Phys. **137**, 134113 (2012).
- [27] X. Laforgue, G. Dridi, S. Guérin, Optimal robust quantum control against pulse inhomogeneities: Analytic solutions, Phys. Rev. A (2022).
- [28] IBM Quantum. <https://quantum-computing.ibm.com/>
- [29] P. Krantz, M. Kjaergaard, F. Yan, T.P. Orlando, S. Gustavsson, and W.D. Oliver, A quantum engineer's guide to superconducting qubits, App. Phys. Rev. **6**, 021318 (2019).
- [30] E. A. Shapiro, V. Milner, C. Menzel-Jones, and M. Shapiro, Piecewise Adiabatic Passage with a Series of Femtosecond Pulses, Phys. Rev. Lett. **99**, 033002 (2007).
- [31] J.A. Vaitkus and A.D. Greentree, Digital three-state adiabatic passage, Phys. Rev. A **87**, 063820 (2013).
- [32] I. Paparella, L. Moro, and E. Prati, Digital stimulated Raman passage by deep reinforcement learning, Phys. Lett. A **384**, 126266 (2020).
- [33] J.A. Vaitkus, M.J. Steel, and A.D. Greentree, Digital waveguide adiabatic passage part 1: theory, Opt. Express **25**, 5466 (2017); V. Ng, J.A. Vaitkus, Z.J. Chaboyer, T. Nguyen, J.M. Dawes, M.J. Withford, A.D. Greentree, and M.J. Steel. Digital waveguide adiabatic passage part 2: experiment, *ibid.* **25**, 2552 (2017).
- [34] T. Alexander, N. Kanazawa, D.J. Egger, L. Capelluto, C.J. Wood, A. Javadi-Abhari, and D. McKay, Qiskit pulse: programming quantum computers through the cloud with pulses, Quantum Sci. Technol. **5**, 044006 (2020).

- [35] G. Aleksandrowicz et al., Qiskit: An Open-source Framework for Quantum Computing (2019); <https://doi.org/10.5281/zenodo.2562111>
- [36] A. Garon, S. J. Glaser, and D. Sugny, Time-optimal control of SU(2) quantum operations, *Phys. Rev. A* **88**, 043422 (2013).
- [37] T. Schulte-Herbrüggen, A. Spörl, N. Khaneja, and S. J. Glaser, Optimal control-based efficient synthesis of building blocks of quantum algorithms: A perspective from network complexity towards time complexity, *Phys. Rev. A* **72**, 042331 (2005).